

ENC-2022-0676

NUCLEATE POOL BOILING OF CARBON DIOXIDE ON A HORIZONTAL AND VERTICAL SURFACE

Rafael Boschini Albuquerque Passarella

Thaís Pirez Alves Ferreira

Universidade Federal de Santa Catarina, Programa de Pós-Graduação em Engenharia Mecânica, Florianópolis-SC

rpassarella@lepten.ufsc.br

thais.pirez@posgrad.ufsc.br

Adonis Menezes

Instituto Federal de Santa Catarina, Itajaí-SC

adonis.ifsc@gmail.com

Júlio César Passos

Universidade Federal de Santa Catarina, Departamento de Engenharia Mecânica, Centro Tecnológico, Campus Trindade, Florianópolis-SC

julio.passos@lepten.ufsc.br

Abstract. *The nucleate boiling has as main characteristic the transfer of high heat fluxes to small temperature differences between the heating surface and the refrigerant fluid. This makes possible to design heat exchangers with smaller dimensions due to the high heat transfer coefficients. Carbon dioxide (CO₂) - when treated as a refrigerant fluid is called R-744 - is a natural, abundant, inexpensive, non-toxic and non-flammable fluid, which is harmful to health only at high concentrations (above 1000 ppm in air). However, experimental data for CO₂ nucleate boiling are scarce in the open literature. Thus, in order to comprehend the behavior of carbon dioxide during nucleate boiling, this study presents experimental results on the end of a copper block horizontally and vertically oriented. The dimensions of the end surface of the copper block are 10 mm width and 30 mm height, when vertically oriented. Test conditions include a pressure of 2.8 MPa, density of 727 kg/m³ and heat flux varying from 69 kW/m² to 293 kW/m². The experimental heat transfer coefficient is obtained and compared with values predicted by models in the literature.*

Keywords: Pool boiling, Nucleate boiling, Carbon dioxide, R744.

1. INTRODUCTION

Carbon dioxide, also known as R744 in the refrigeration industry, is a long known natural cooling fluid, whose thermophysical properties enable its application with low to no impact to the environment. Despite its low GWP (global warming potential), null ODP (ozone depletion potential), non-flammability and non-toxicity, it has been substituted by chlorofluorocarbons (CFCs), hydrochlorofluorocarbons (HCFCs) and hydrofluorocarbons (HFCs), that are able to operate in lower pressures than CO₂. However, after the pressure exerted by international treaties for the mitigation of human impacts, such as the Montreal Protocol, carbon dioxide has gained renewed interest in its applicability.

Nowadays, carbon dioxide is used from automotive air conditioning, residential heat pumps to small electronic devices, among other high heat transfer removal systems. Nonetheless, the different physical and transport properties of CO₂, when compared to traditional cooling fluids, have significant impact on the evaporation process, thus requiring further research concerning its heat transfer capability and potential.

The nucleate pool boiling, commonly encountered in flooded evaporators for example, is among the themes concerning this fluid that need further research. This mode of heat transfer happens when a body, fully immersed in an extensive pool of stationary liquid, has boiling occurring in its surface. This process can be influenced by several parameters, such as: heat flux, thermophysical properties of the fluid, surface and finish of the immersed material and size of the heated surface. Due to the distinct thermophysical characteristics of carbon dioxide, this is a subject that has not been profoundly explored in the literature.

Loebl, Kraus and Quack (2005) explored the pool boiling of carbon dioxide on a horizontal surface, with pressuring ranging from 0.53 to 1.43 MPa, temperatures from -56 to -30 °C and heat fluxes up to 80 kW/m². The

authors further investigated the influence of wall material and roughness on the pool boiling heat transfer. They were first to publish data concerning the use of stainless steel and aluminum as wall material for carbon dioxide pool boiling. The authors were able to conclude that there is indeed an exceptional influence of the wall material, but it is not as large as described for other refrigerants. Loebel, Kraus and Quack (2005) were able to perceive that the heat transfer coefficient on a stainless steel tube is about 70% of that on a copper tube and this value increases to 87% for aluminum; however, they were not able to identify the reason behind the influence of the wall material. The data obtained for copper tubes agree with those encountered in other researches and accepted correlations.

Gorenflo and Kotthoff (2005) published a review on pool boiling of carbon dioxide, discussing the state of the art of the time. The authors explained that the reason that CO₂ has higher heat transfer coefficient when compared to hydrocarbons or halocarbons refrigerants is due to the higher reduced saturation pressure of its application, not because it has extraordinary thermophysical properties. They explained that the influence of wall material (considering tubes with the same surface treatment) is due to a mixed effect of material properties and surface structure. The authors also highlight that carbon dioxide is on par with the trends encountered to other fluids concerning the dependence of the heat transfer coefficient on heat flux and reduced pressures. They concluded by remarking that CO₂ has indeed higher heat transfer capabilities than other refrigerants at the same saturation temperature.

Gorenflo et al. (2014) presented a state-of-the-art review about the prediction methods for pool boiling. They highlighted that the predictive methods currently used are empirical or semi-empirical, because “theoretically consistent calculation of the heat transfer coefficient is not yet possible”. The authors elaborate that at low to intermediate heat fluxes and reduced pressures, heaters with plain surfaces are less efficient than those with fins (integral, trapezoid-shaped or “k-shaped”). They also performed a comparison of eight predictive methods with the method and experimental data of the Heat Atlas (Gorenflo and Kenning, 2010; Gorenflo, 2013). The methods with lower relative deviations of heat transfer coefficient values of carbon dioxide on copper heaters are those by Shekrladze (2008): 0.00% of deviation; Heat Atlas (Gorenflo and Kenning, 2010; Gorenflo, 2013): -2.73% of deviation and Ribatski and Saiz Jabardo (2003): -7.64% of deviation. The authors conclude by highlighting the need for improvement of the knowledge concerning the influence of the heater and more accurate experimental data on surface tension, this will allow for better elucidation concerning the influence of thermophysical properties of the fluid.

Lin and Kedzierski (2019) reviewed the pool boiling heat transfer of low GWP fluid on enhanced surfaces. The usage of this type of surface in conjunction with low GWP fluids allows for a smaller charge of cooling fluid, reducing the risks associated with it, as well as increasing the efficiency of the equipment. Commonly used enhanced surfaces, “generally features reentrant cavities with connecting tunnels and mouth opening smaller than the cavity”. The authors did not find an extensive quantity of studies concerning NH₃ and CO₂ in the literature, however, they stated that enhanced surfaces lead to noteworthy improvement in the pool boiling of this kind of fluid, with enhancement factors varying from 1 to 10, depending on the enhancement geometry and the cooling fluid.

Liu et al. (2020) proposed a correlation for the boiling heat transfer coefficient of CO₂ on the external surfaces of evaporating tubes. The authors analyzed the heat transfer capability of a smooth tube and three enhanced geometries. They were able to perceive an increase of the heat transfer coefficient with the increase of the heat flux and pressure. However, for higher heat fluxes, there was a decrease of the wall superheating effect. In accordance with Lin and Kedzierski (2019), the authors also described higher heat transfer coefficients for the enhanced surfaces, when compared with the smooth tube (same heat flux). Among the enhanced surfaces, the finned tube presented a faster increase of the heat transfer coefficient, due to the extra area of the fins – which is in agreement with Gorenflo et al. (2014). Liu et al. (2020) concluded that “the special structures of mechanically enhanced tube surface are favorable for the formation and maintenance of vaporization cores and for expelling gas bubbles”. The authors assessed that the heat transfer coefficient is proportional to the geometric parameters of the tube, and the enhancement factors can also be considered a function of such parameters.

Overall, the research concerning carbon dioxide pool boiling heat transfer still lack experimental data for the heat transfer coefficient. Thus, in this study, the pool boiling of CO₂ over a horizontal and vertical copper surface was investigated. The test was conducted at the saturation pressure of 2.8 MPa and heat flux varying of 69 kW/m² to 293 kW/m².

2. EXPERIMENT

2.1 Experimental set up

The experimental set up is schematically presented in Fig. 1. It consists of (1) a pressurized chamber, (2) two thermal baths, for temperature control, (3) one power source, (4) one data acquisition system and (5) one computer. It also includes a controller of CO₂ in the air, for safety reasons.

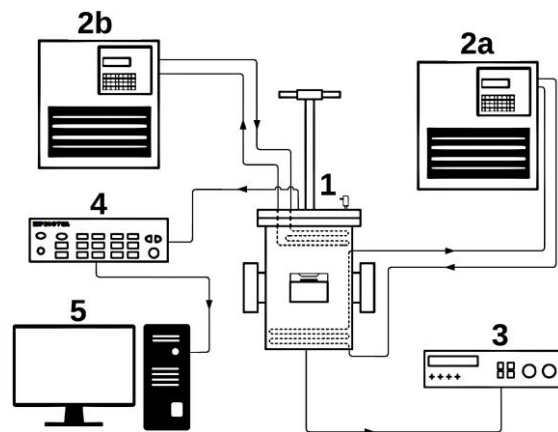


Figure 1. Schematic of the experimental apparatus

The pressurized chamber, Fig. 2, is made of AISI 316 stainless steel inside which the test section is placed, immersed in the liquid region of the working fluid. The chamber has an internal diameter of 230 mm and a height of 240 mm, with a volumetric capacity of 11 liters.

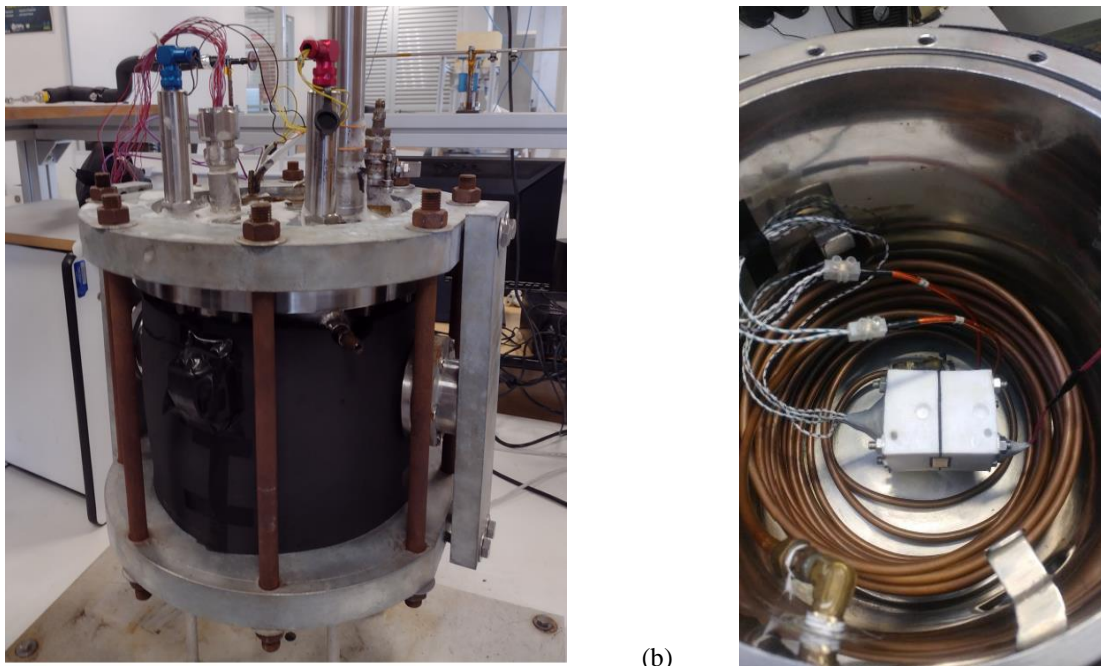


Figure 2. Pressurized Chamber: (a) outside view and (b) internal view.

On the top of the chamber there are two temperature transmitters, one pressure transmitter, one feedthrough for the thermocouples (manufactured by Conax technologies), one charging valve and two pressure relief valves calibrated to open at 7.0 MPa. At the bottom of the chamber there is one feedthrough for the current cables. Inside the chamber there are two serpentes of copper to control the CO₂ temperature and the test section. Figure 2 (b) shows inside the chamber.

2.2 Test section

The test section showed in Fig. 3 (a) consists of a block of electrolytic copper which is insulated by a Teflon box over its entire surface except for the front part of 10 mm of width and 30 mm of length. There are two cartridge electrical resistances inside the copper block, assembled inside the hollows showed in Fig. 3 (b), with diameter of 11.1 mm and 50 mm of length. Each of them with 10 ohms and capable to supply up to 250 W of power.

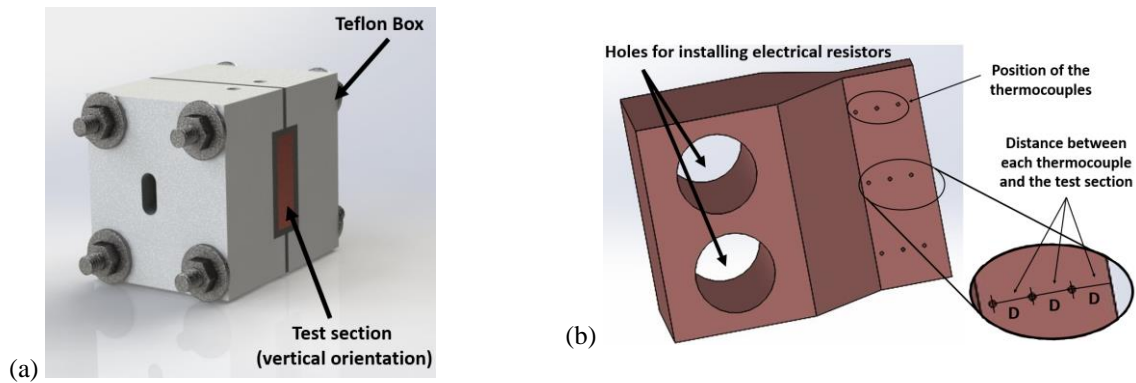


Figure 3. (a) Test section and (b) position of the thermocouples on the copper block, where D is equal to 3 mm.

The block of electrolytic copper has nine thermocouples positioned at the end part of the copper block, which has a constant cross section area of 10 mm of width and 30 mm of height, when vertically oriented, as showed in Fig. 3 (b). Each thermocouple has 3 mm of distance between the edge of the block and between the next thermocouple on the same line, as showed in the Fig. 3 as the letter D . The thermocouples are positioned 5 mm inside the block.

2.3 Experimental procedure

The experimental procedure started with the assembling of the test section. The cartridge electrical resistances are positioned by a thermal paste (conductivity $k = 0.4 \text{ W/mK}$). The thermocouples are positioned and fixed in the copper with the aid of glue. The pressure of the Teflon box holds them in place. The output cables from the thermocouples and from the resistances are sealed using epoxy resin. Two O-rings are positioned, one around the copper block and the two halves of the Teflon box and the second one around the final part of the copper block, where the boiling occurs. Then, a first treatment was made in the milling cutter to eliminate any high differences between the cooper, the O-ring and the Teflon box. The boiling surface used is treated with a sandpaper with mesh size of 1200 and a final treatment with a mesh size of 2000.

The test section is then positioned inside the pressurized chamber and a compressed air test is done to check for leakages. After that vacuum is made and the pressure chamber is charged with a small quantity of CO_2 , enough to reach the pressure of 3.0 MPa, which is above the test pressure. The chamber had its pressure monitored over 24 hours in order to verify if there were any small leakages that were not identified before. As the amount of CO_2 inside is very low, any small leakage will cause a visible pressure drop.

The charging process was carried out once it was concluded that the chamber did not have any leakage. Insulating blanket was then placed around the entire pressure chamber, as showed in Figure 4, and vacuuming was done on the chamber. The thermal baths had their temperature set to 243 K and, with help of a scale, 8 kg of CO_2 were loaded into the pressurized chamber. For this load a pressure regulator valve was used. As the chamber has 11 liters of volumetric capacity, the density is 727 kg/m^3 . With this density and pressure, the saturation state, and the liquid column higher than the test section were guaranteed conditions. The thermal baths had their temperature set to around 255 K to equilibrate the internal pressure of around 2.8 MPa.



Figure 4. Pressurized chamber with the insulating blanket

The power supply responsible for feeding the test section resistors was turned on and the test was carried out for heat fluxes of 69 kW/m^2 to 293 kW/m^2 . With the increase of the heat flux, considering the room temperature constant at 294 K , it was necessary to remove more heat from the fluid refrigerant to keep the pressure (2.8 MPa) and saturation temperature (265.12 K) constants, thus with the increase of the heat flux, the temperature set in the thermal baths were decreased. In order to verify the stability of the system during a representative test, for a heat flux of 251 kW/m^2 , a sample of 60 points for the instantaneous pressure signal was acquired and is shown in Figure 5. The maximum variation was of 0.003 MPa .

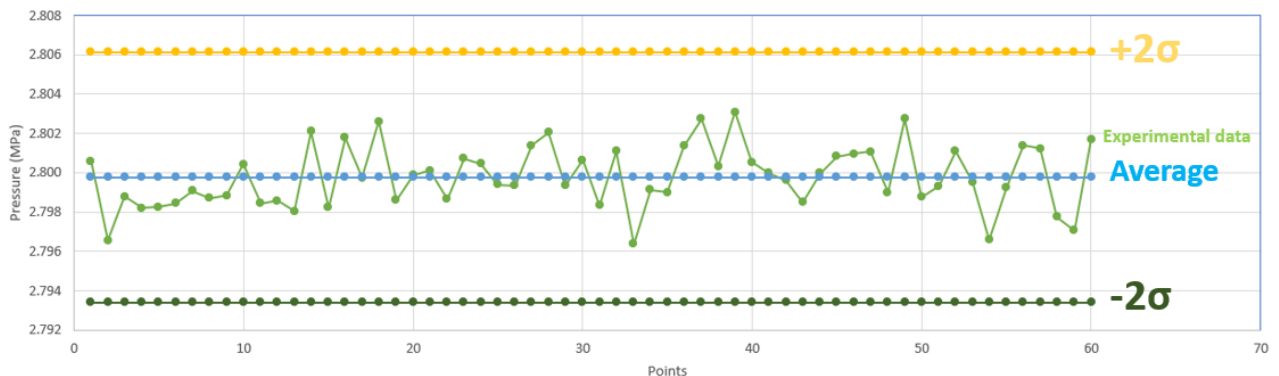


Figure 5. Instantaneous pressure variation along the 60 collected points, $q'' = 251 \text{ kW/m}^2$.

Tests were conducted by gradually increasing the heat flux up to a maximum and then gradually reduced. The lowest heat flux point was where the temperature difference between each sequential thermocouple was greater than the temperature uncertainty. The critical flux of Zuber was calculated following the guidelines in Carey (1992) and was observed to be about 780 kW/m^2 , much smaller than the heat fluxes used, but simulations showed that for a temperature of 300 K in the thermocouples the temperature near the resistors would be much higher. Therefore, the maximum heat flux limit was imposed as the one that wouldn't pass the temperature of 300 K on the thermocouple closest to the resistors. Only the upward heat flux data were considered for analysis purposes.

Three values of heat fluxes were calculated by the application the Fourier law in one direction, considering the three thermocouples on the same line. The average of these heat fluxes was around 5% less than the one calculated with the tension and current from the power supply. Simulations on ANSYS have shown a virtually negligible convection loss on the Teflon surface. This loss may be associated with a bad thermal paste, which is present between the cartridge heaters and the copper block. Considering this, the heat transfer coefficient calculation was done with the average heat flux calculated from the thermocouples. An average for the wall temperature was also made considering the three thermocouples and their corresponding distance to the wall, also by Fourier law. The copper thermal conductivity was considered constant $400 \text{ W/m}^2\text{K}$.

Instruments were calibrated and the uncertainty of measured parameters are given in Tab. 1.

Table 1. Uncertainty of measured and calculated parameters

Parameter	Orientation	Heat flux, q'' (kW/m ²)	Uncertainty
Heat transfer coefficient, h (kW/m ² K)	horizontal	96	± 26 %
	horizontal	293	± 7 %
	vertical	96	± 26 %
	vertical	250	± 8 %
Wall temperature	-	-	± 0.2 K
Saturation temperature	-	-	± 0.1 K

3. RESULTS AND CORRELATION COMPARISONS

The experimental results for the heat transfer coefficient (HTC) obtained in this study are presented in Fig. 6. As expected, the heat transfer coefficient is higher in the vertical surface in comparison with the horizontal surface. For the horizontal surface the HTC showed a decline in the curve after the 200 kW/m² point, while the vertical surface was still increasing. The reasons are yet to be investigated.

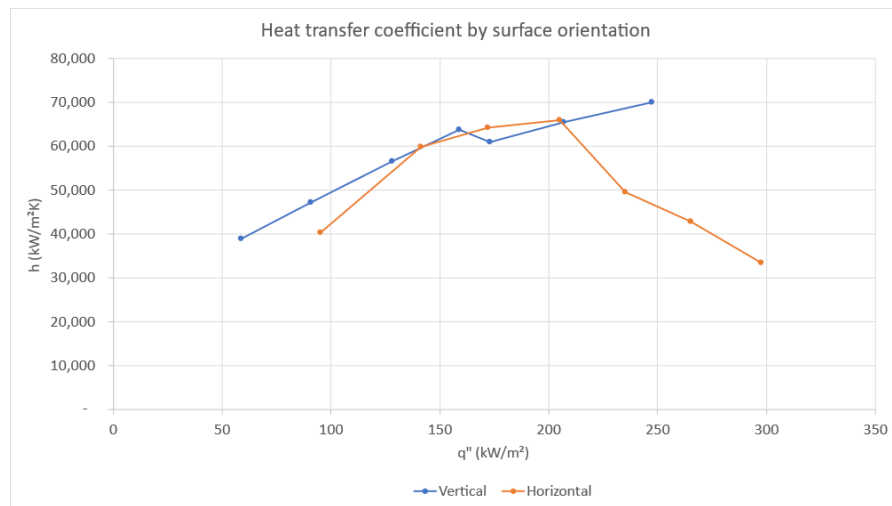


Figure 6. Heat transfer coefficient x heat flux curve for vertical and horizontal surfaces.

The results were compared with eight empirical correlations available in the literature. Table 2 presents these equations in which the only the first two have CO₂ in their databases. The surface orientation was on the external surface of horizontal tubes, for Eqs. (1) to (7).

The correlation of Gorenflo (1986), apud. Kandlikar (1999), Eq. (1), is a function of the reduced pressure $p^* = (P/P_c)$, where P and P_c represent the pressure and the critical pressure, respectively, with a reference HTC $h_0=2200$ W/m²K for $q_0''=2 \times 10^4$ W/m². Liu et al. (2020) presented a correlation that is function of the reduced pressure as well, and the heat flux for smooth tubes. For Eq. (3) was used C_4 as 3.8. Eq. (5) is Kutateladze (1966) original correlation and Eq. (6) is his modified one.

Table 2. Correlations

Author	Correlations	Equation
Gorenflo (1986)	$\frac{h}{h_0} = \left(\frac{q''}{q''_0}\right)^{(0.9-0.3p^{*0.3})} 2.1p^{*0.27} + \left(4.4 + \frac{1.8}{1-p^*}\right)p^*$	(1)
Liu et al. (2020)	$h = 915.5248p^{*3.4832}q''^{(2.3892-2.0348p^{*0.1405})}$	(2)
Stephan and Abdelsalam (1980)	$h = C_4 q''^{0.745}$	(3)
Kutateladze (1990) apud. Piore, Rohsenow and Doerffer (2004)	$h = \left[3.37 \times 10^{-9} \frac{k_l}{L^*} \left(\frac{h_{lv}}{c_{pl} q''}\right)^{-2} \left(\frac{\rho_l}{\rho_v}\right)^{-2} \left(\frac{\rho_l - \rho_v}{\sigma g}\right)^4 \right]^{1/3}$	(4)
Kutateladze (1966) apud. Piore, Rohsenow and Doerffer (2004)	$\frac{hL^*}{k_l} = 0.44 \left(\frac{1 \times 10^{-4} q'' P}{g h_{lv} \rho_v \mu_l} \frac{\rho_v}{\rho_l - \rho_v}\right)^{0.7} Pr_l^{0.35}$	(5)
Labunsov (1972) apud. Piore, Rohsenow and Doerffer (2004)	$h = 0.075 \left[1 + 10 \left(\frac{\rho_v}{\rho_l - \rho_v}\right)^{0.67} \right] \left(\frac{k_l}{\nu_l \sigma T_{sat}}\right)^{0.33} q''^{0.67}$	(6)
Kruzhilin (1947 apud. Piore, Rohsenow and Doerffer (2004))	$\frac{hL^*}{k_l} = 0.082 \left(\frac{h_{lv} q''}{g T_{sat} k_l} \frac{\rho_v}{\rho_l - \rho_v}\right)^{0.7} \left(\frac{T_{sat} c_{pl} \sigma \rho_l}{h_{lv}^2 \rho_v^2 L^*}\right)^{0.33} Pr_l^{-0.45}$	(7)
Rohsenow (1952 apud Piore, Rohsenow and Doerffer (2004))	$\frac{c_{pl} \Delta T}{h_{lv}} = C_{sf} \left[\frac{q''}{\mu_l h_{lv}} \sqrt{\frac{\sigma}{g(\rho_l - \rho_v)}} \right]^{0.33} \left(\frac{c_{pl} \mu_l}{k_l}\right)^n$	(8)

For the ensemble of correlations in Tab. 2 and the respective symbols, we have: h is the heat transfer coefficient (W/m^2K), q'' is the heat flux (W/m^2), p^* is the reduced pressure, k_l is the liquid phase conductivity (W/mK), L^* is the pool boiling characteristic length (or capillary length scale) (m), h_{lv} is the vaporization enthalpy (J/kg), c_{pl} is the specific heat at constant pressure of the liquid phase (J/kgK), ρ is the density (kg/m^3), with l indicating the liquid phase and v , the vapor phase, σ is surface tension (N/m), g is the gravitational constant (the value $9.76 m/s^2$ was used, considering the tests were made at Florianópolis, Santa Catarina); Pr is the Prandtl number, ν is the kinematic viscosity (m^2/s); μ is the dynamic viscosity ($Pa \cdot s$); P is the pressure (Pa); T_{sat} is the saturation temperature (K); T_w is the wall temperature and ΔT is the surface superheat ($T_{sat} - T_w$).

Piore, Rohsenow and Doerffer (2004) argued that there are two typical approaches used to determine the heat transfer coefficient for the boiling process, the first approach is “characterized by using constant values for coefficients and powers”, while the second approach is “based on the variability of the coefficients in a correlation according to the surface-fluid combination or the power values depending on the fluid type”.

The Kutateladze, Labunsov and Kruzhilin correlation presented in Tab. 2 are examples of the first approach. It has as the main advantage the “wide range of applicability of the correlations, regardless of the kind of fluid and boiling surface, however the prediction accuracy of this approach may be sacrificed”, as explained by Piore, Rohsenow and Doerffer (2004). These correlations were the ones that presented the highest associated error. For the second approach, the prediction accuracy is better when compared to the first approach, but the surface-fluid interaction is needed in order to use the correlation, which was not available for the experiments performed.

Nonetheless the C_{sf} for the Rohsenow correlation, showed in Eq. (8) of Tab. 2, was calculated, considering $n = 1.7$. For all experimental points the mean C_{sf} was 0.073. However, the 3 higher heat flux for the horizontal orientation showed an increasing value of C_{sf} . Thus, the mean C_{sf} was also calculated without these 3 last points and it was equal to 0.059.

For future studies, the need for further investigation of the impact of surface material in a CO₂ pool boiling is required. With this, a better definition of C_{sf} and consequently, higher accuracy of heat transfer coefficient prediction, will be possible.

The experimental results compared with the cited correlations are displayed in Fig. 7 and Fig. 8, for the horizontal and vertical orientations, respectively.

One can observe that none of the correlations could predict the actual heat transfer coefficient, with emphasis for the horizontal correlations, for which no correlation captured the behavior of the heat transfer coefficient with the heat flux.

However, the behavior of the heat transfer coefficient with the heat flux was well captured for the vertical orientation by the predictive correlations, even though none was accurate on the values. One may suggest that the difference between fluids and surfaces, the finish of the material and size of the heated surface, operating pressure range and especially heat flux range may be responsible for the inaccuracy of the predictions.

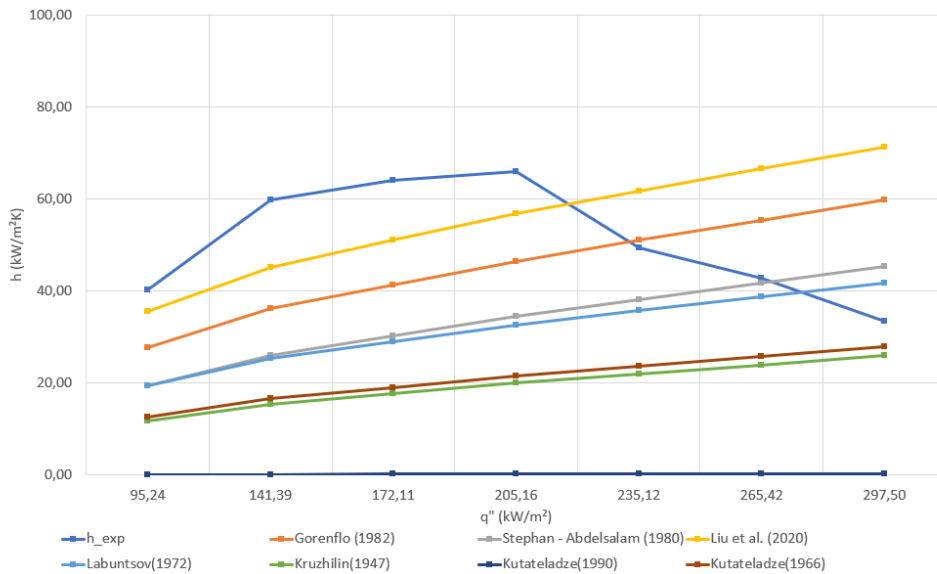


Figure 7. Horizontal Orientation – comparison with correlations

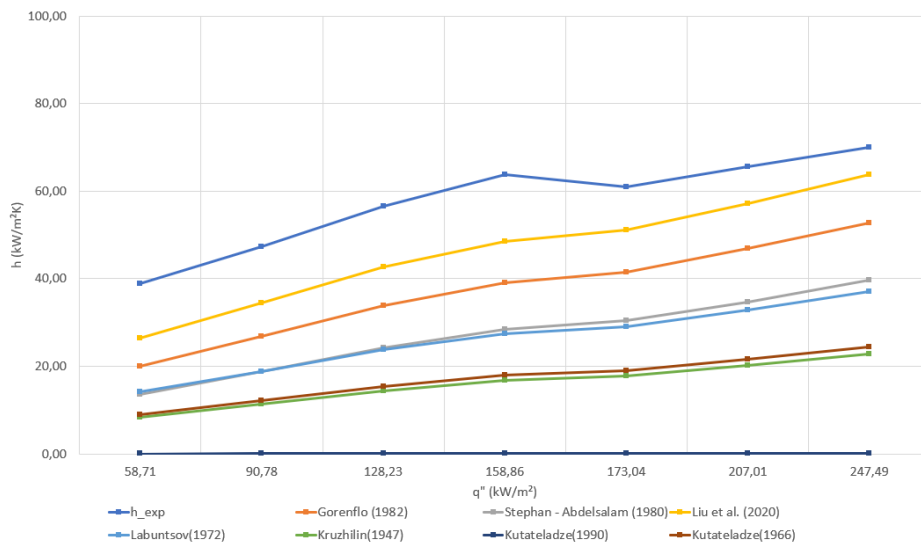


Figure 8. Vertical Orientation – comparison with correlations

Overall, the correlation proposed by Liu et al. (2020) was the one that had the best results. The authors developed their correlation for carbon dioxide evaporating outside copper tubes, which increases the similarities with the tests performed. The correlation is a function of the reduced pressure and heat flux. It was proposed for pressures of 2 to 4 MPa, heat flux of 10 to 50 kW/m² and circular channels (the authors considered diameters of 19 to 22.86 mm). The heat flux is explicit in the correlation; thus the higher values of the test (60 to 293 kW/m²) may be the main responsible for the differences between experimental and predicted heat transfer coefficients. The accuracy of Liu et al. (2020) correlation is displayed in Fig. 9 and Fig. 10, for the horizontal and vertical orientations, respectively.

For both orientation, Liu et al. (2020) correlation predicted 42.8% of the data within $\pm 30\%$ error band. The minimum prediction error was -12.02% for the horizontal surface and 9.74% for the vertical surface. The maximum prediction error were 76.95% for the horizontal and 64.26% for the vertical. However, the last three experimental points for horizontal plate, in which a decrease of the heat transfer coefficient can be observed, need to be revised. It's important to emphasise the high complexity of the experimental work during pool boiling of CO₂ is an additional challenge for obtaining data points, and this is one of the main factors for the scarcity of experimental literature.

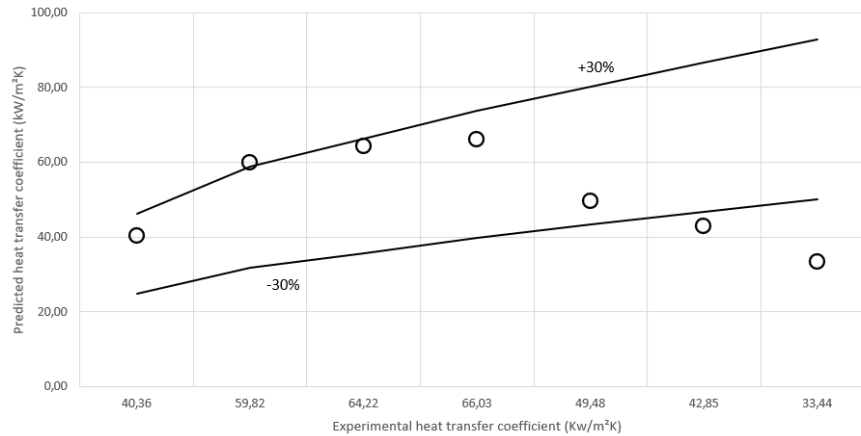


Figure 9. Accuracy of Liu et al. (2020) correlation in the horizontal orientation

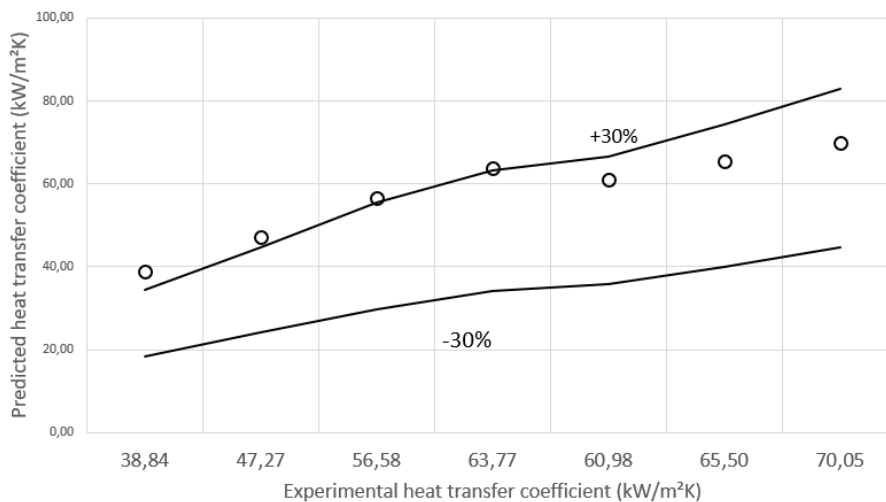


Figure 10. Accuracy of Liu et al. (2020) correlation in the vertical orientation

The accuracy of the predictive correlations presented in Tab. 2 were calculated by subtracting the experimental heat transfer coefficient from the predicted value and dividing the result by the experimental coefficient. The predicted error varies and tends to rise with increasing heat flux, which does not align with the literature, therefore, more investigation needs to be done.

4. CONCLUSIONS

Experimental results on nucleate CO₂ pool boiling on a vertical and horizontal copper surface were presented. In the absence of surface roughness, correlations that were dependent on the surface-fluid and with fixed power and coefficients were applied.

The heat transfer coefficient trend was well captured by the selected correlations for the vertical orientation, however, none was accurate on the values. For the horizontal orientation, the heat transfer coefficient value and trend were not captured by the predictive correlation and the reasons will be investigated. The correlation proposed by Liu et al. (2020) had the best results. It predicted 42.8% of the data within $\pm 30\%$ error band. It's important to emphasize that this correlation considered CO₂ in its database, and it was obtained for boiling on the external surface of a horizontal tube.

The predicted error varies and tends to rise with increasing heat flux, which is not in accordance with the literature, therefore, more investigation needs to be done.

It can be concluded that there is a need for further comprehension on the pool boiling phenomena of the carbon dioxide, specially at flat surfaces – which is not a common occurrence on the literature. The impacts of surface's roughness, fluid/surface combination and surface's orientation are topics for future studies.

5. ACKNOWLEDGEMENTS

The authors gratefully acknowledge the partial support of this work by Brazilian National Council of Research (CNPq), by CAPES Foundation and an ANEEL-PETROBRAS project to improve the laboratory infrastructure.

6. REFERENCES

- Carey, V. P. "Liquid-vapor phase-change phenomena: an introduction to the thermophysics of vaporization and condensation processes in heat transfer equipment". Taylor & Francis. 1992.
- Gorenflo, D., 2013. *VDI-Wärmeatlas*. Springer, Berlin, Heidelberg, 11th edition.
- Gorenflo, D., Baumhögger, E., Herres, G. and Kotthoff, S., 2014. "Prediction methods for pool boiling heat transfer: A state-of-the-art review." *International Journal of Refrigeration*, Vol. 43, pp. 203-226.
- Gorenflo, D., Knabe, V., & Bieling, V. 1986. "Bubble Density on Surfaces with Nucleate Boiling-Its Influence on Heat Transfer and Burnout Heat Flux at Elevated Saturation Pressures." In International Heat Transfer Conference Digital Library. Begel House Inc.
- Gorenflo, D., Kotthoff, S., 2005. "Review on pool boiling heat transfer of carbon dioxide." *International Journal of Refrigeration*, Vol. 28, No. 8, pp. 1169-1185.
- Gorenflo, D., Kenning, D.B.R., 2010. *VDI- Heat Atlas*. Springer, Berlin, 2nd edition.
- Kandlikar, S. G. Handbook of phase change: boiling and condensation. 1999. Taylor & Francis, Philadelphia, 1st ed.
- Kruzhilin, G.N. 1947. "Free-convection transfer of heat from a horizontal plate and boiling liquid". *Doklady AN SSSR* (Reports of the USSR Academy of Sciences), Vol. 58, No.8, pp.1657–1660 (in Russian).
- Kutateladze, S.S, Borishanskii, V.M. 1966. A Concise Encyclopedia of Heat Transfer, Pergamon Press, New York, NY.
- Kutateladze, S.S. 1990. Heat Transfer and Hydrodynamic Resistance: Handbook, Energoatomizdat Publishing House, Moscow.
- Labuntsov, D.A. 1972. "Heat transfer problems with nucleate boiling of liquids", *Thermal Engineering*, Vol. 19, No.9, pp.21–28.
- Lin, L., Kedzierski, M. A., 2019. "Review of low-GWP refrigerant pool boiling heat transfer on enhanced surfaces." *International Journal Of Heat And Mass Transfer*, Vol. 131, pp. 1279-1303.
- Liu, S., Qi, H., Nian, V., Liu, B., Dai, B. et al. 2020. "A new correlation for carbon dioxide boiling heat transfer coefficient outside evaporating tubes." *Journal of Cleaner Production*, Vol. 276, pp. 123050.
- Loebl, S.; Kraus, W. E.; Quack, H., 2005. "Pool boiling heat transfer of carbon dioxide on a horizontal tube." *International Journal Of Refrigeration*, Vol. 28, No. 8, pp. 1196-1204.
- Pirola, I. L., Rohsenow, W., & Doerffer, S. S. 2004. "Nucleate pool-boiling heat transfer. II: assessment of prediction methods". *International Journal of Heat and Mass Transfer*, Vol.47, No.23, pp.5045-5057.
- Ribatski, G. and Jabardo, J. M. S., 2003. "Experimental study of nucleate boiling of halocarbon refrigerants on cylindrical surfaces." *International Journal Of Heat And Mass Transfer*, Vol. 46, No. 23, pp. 4439-4451.
- Rohsenow, W.M. (1951) "A method of correlating heat transfer data for surface boiling of liquids", Transactions of the ASME 74 (1952) 969–976.
- Shekriladze, I. G., 2008. "Boiling heat transfer: mechanisms, models, correlations and the lines of further research." *The Open Mechanical Engineering Journal*, Vol. 2, No. 1.

7. RESPONSIBILITY NOTICE

The authors are the only responsible for the printed material included in this paper.